Electronic Supplementary Information (ESI) for

Construction of Soft Nanoporous Crystal with Silole Derivative: Strategy of Framework Design, Multiple Structural Transformability and Mechanofluorochromism

Ju Mei,[a] Jian Wang,[a] Anjun Qin,[a] Hui Zhao,[a] Wangzhang Yuan,[b] Zujin Zhao,[b] Herman H. Y. Sung,[b] Chunmei Deng,[b] Shuang Zhang,[a] Ian D. Williams,[b] Jing Zhi Sun,*[a] and Ben Zhong Tang*[a,b]

[a] Department of Polymer Science and Engineering, Institute of Biomedical Macromolecules, MOE Key Laboratory of Macromolecular Synthesis and Functionalization, Zhejiang University, Hangzhou 310027, PR China;

[b] Department of Chemistry, The Hong Kong University of Science & Technology, Clear Water Bay, Kowloon, Hong Kong, PR China.

Table of Contents

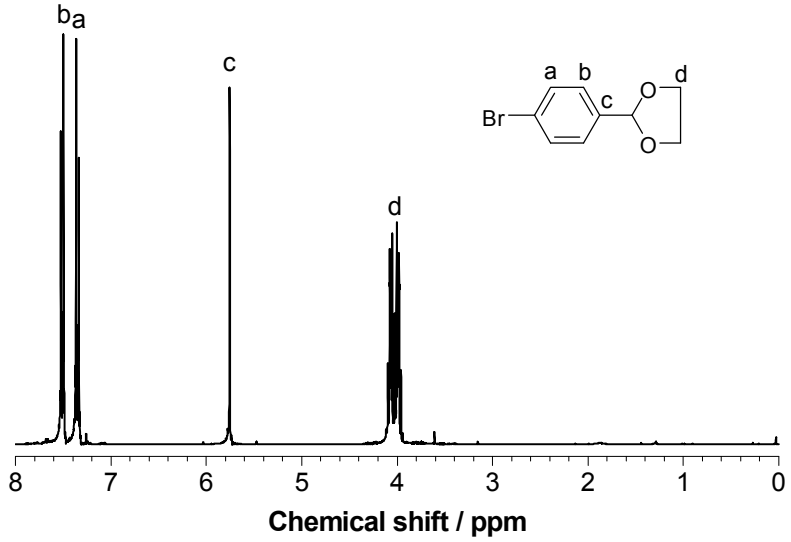

Fig. S1 ^{1}H NMR spectrum of 2-(4-bromophenyl)-1,3-dioxolane (in $CDCl_3$).

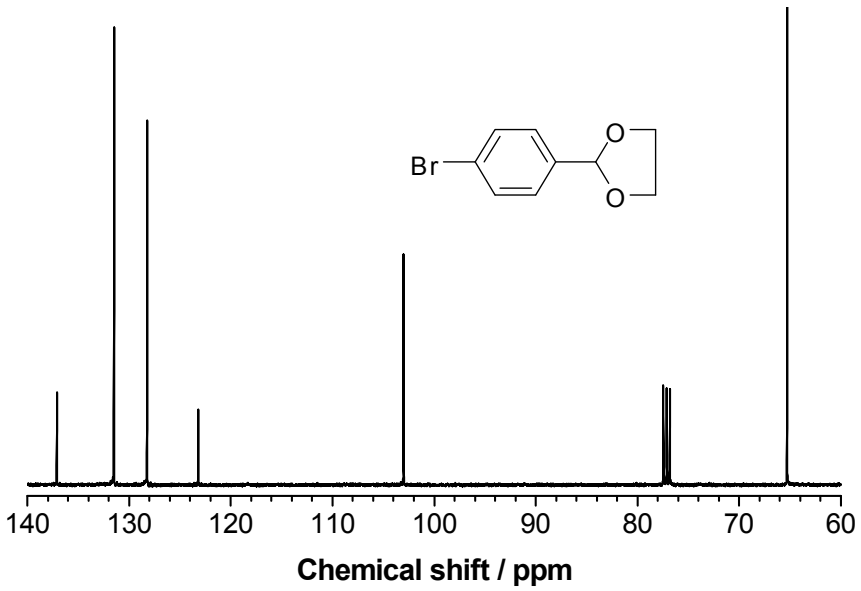

Fig. S2 ^{13}C NMR spectrum of 2-(4-bromophenyl)-1,3-dioxolane (in $CDCl_3$).

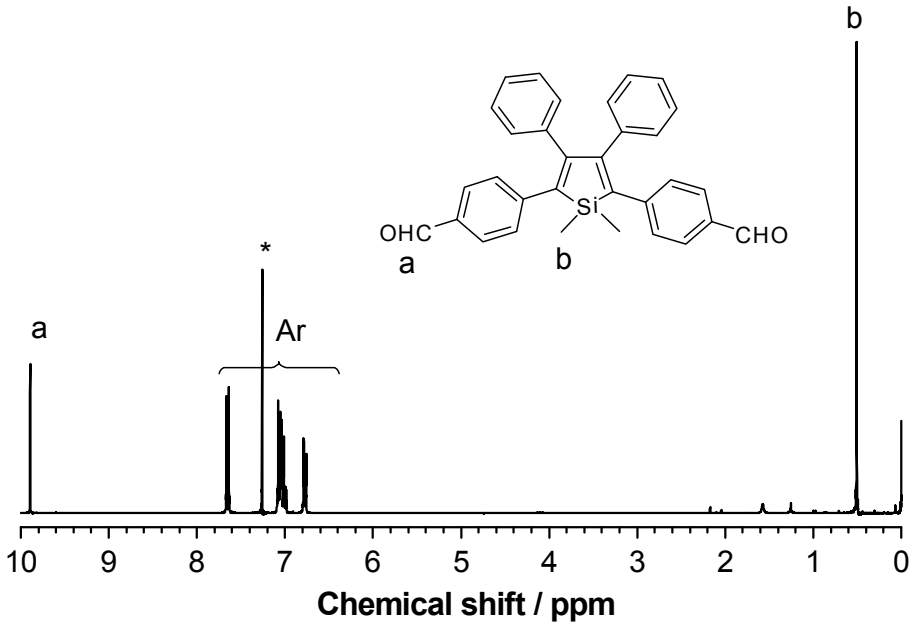

Fig. S3 ^{1}H NMR spectrum of 1,1-dimethyl-2,5-bis(4-benzaldehyde)-3,4-diphenylsilole (in $CDCl_3$). The solvent peaks are marked with asterisks.

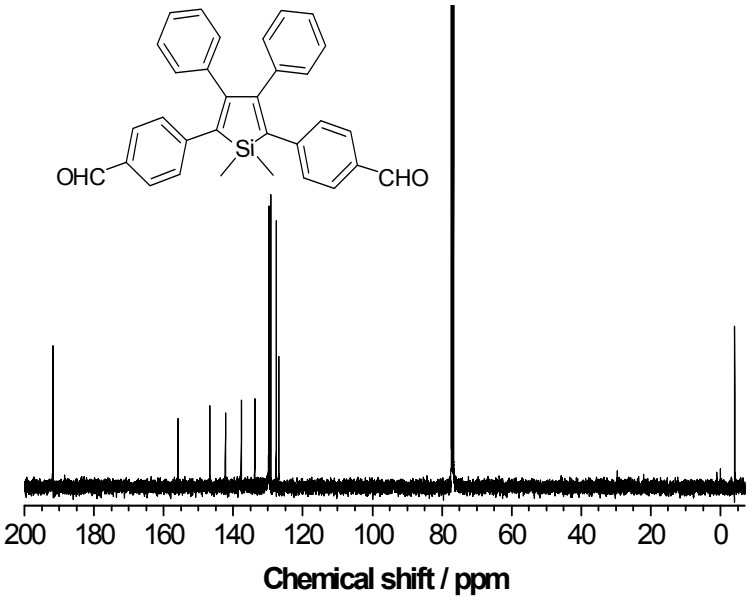

Fig. S4 ^{13}C NMR spectrum of 1,1-dimethyl-2,5-bis(4-benzaldehyde)-3,4-diphenylsilole (in $CDCl_3$).

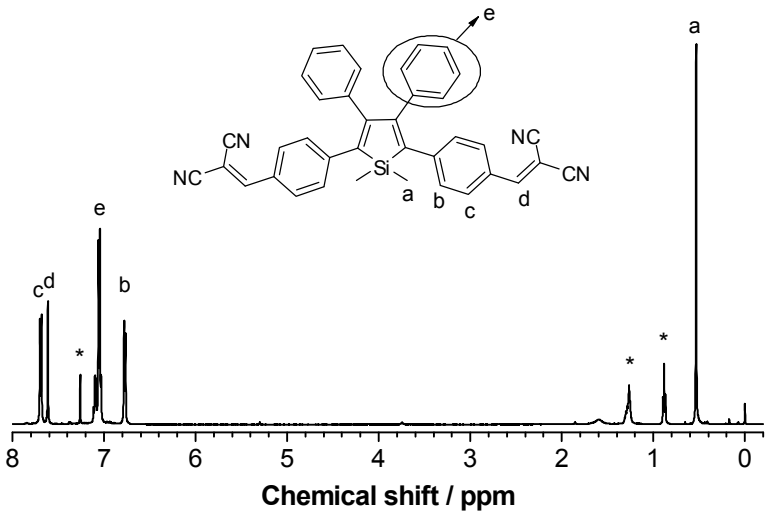

Fig. S5 ^{1}H NMR spectrum of **8** (in $CDCl_3$). The solvent peaks are marked with asterisks.

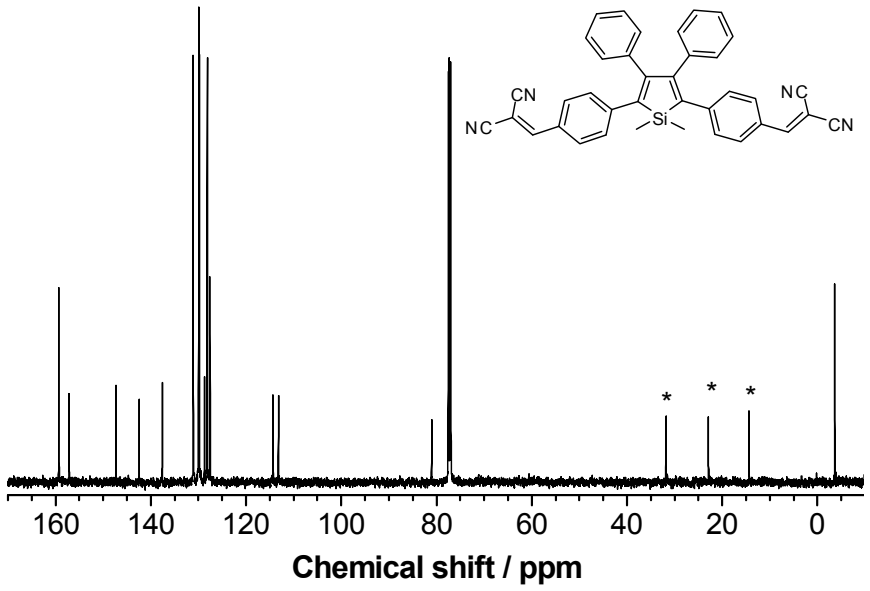

Fig. S6 ^{13}C NMR spectrum of **8** (in $CDCl_3$). The solvent peaks are marked with asterisks.

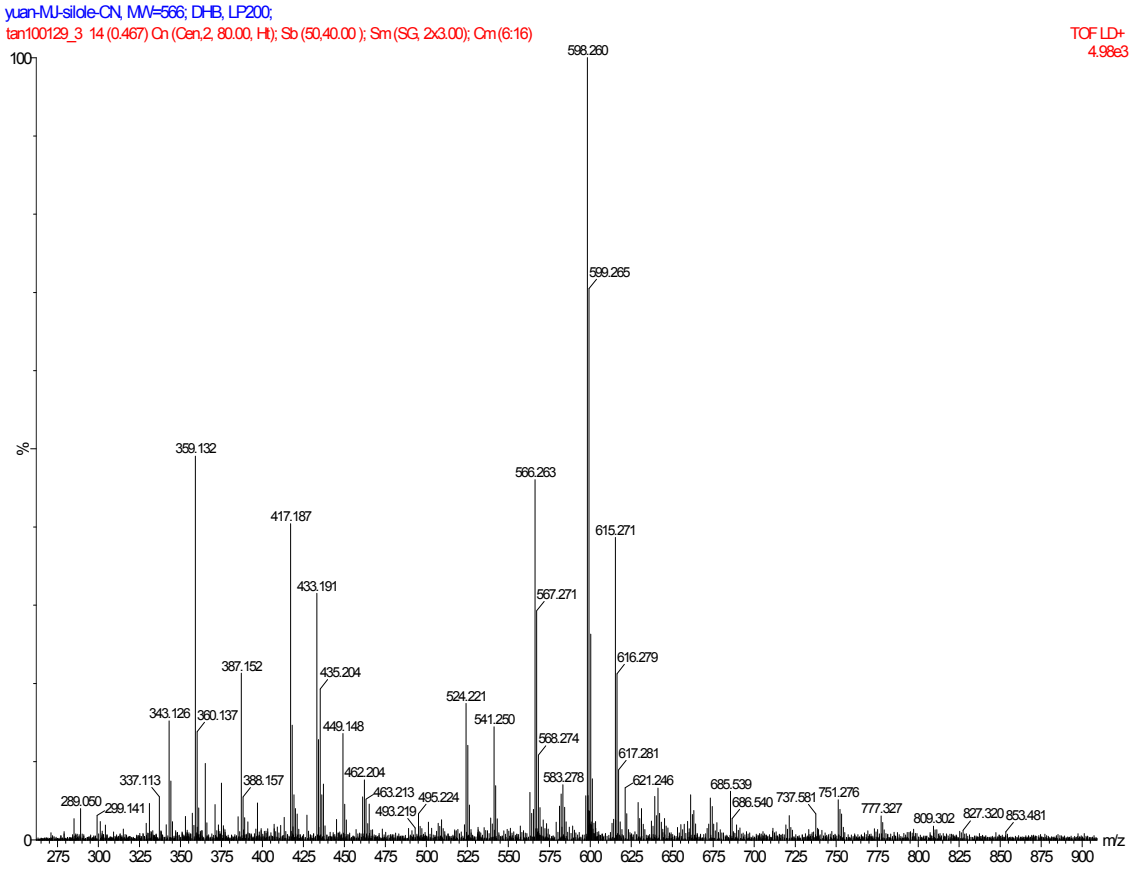

Fig. S7 MALDI–TOF mass spectrum of **8**.

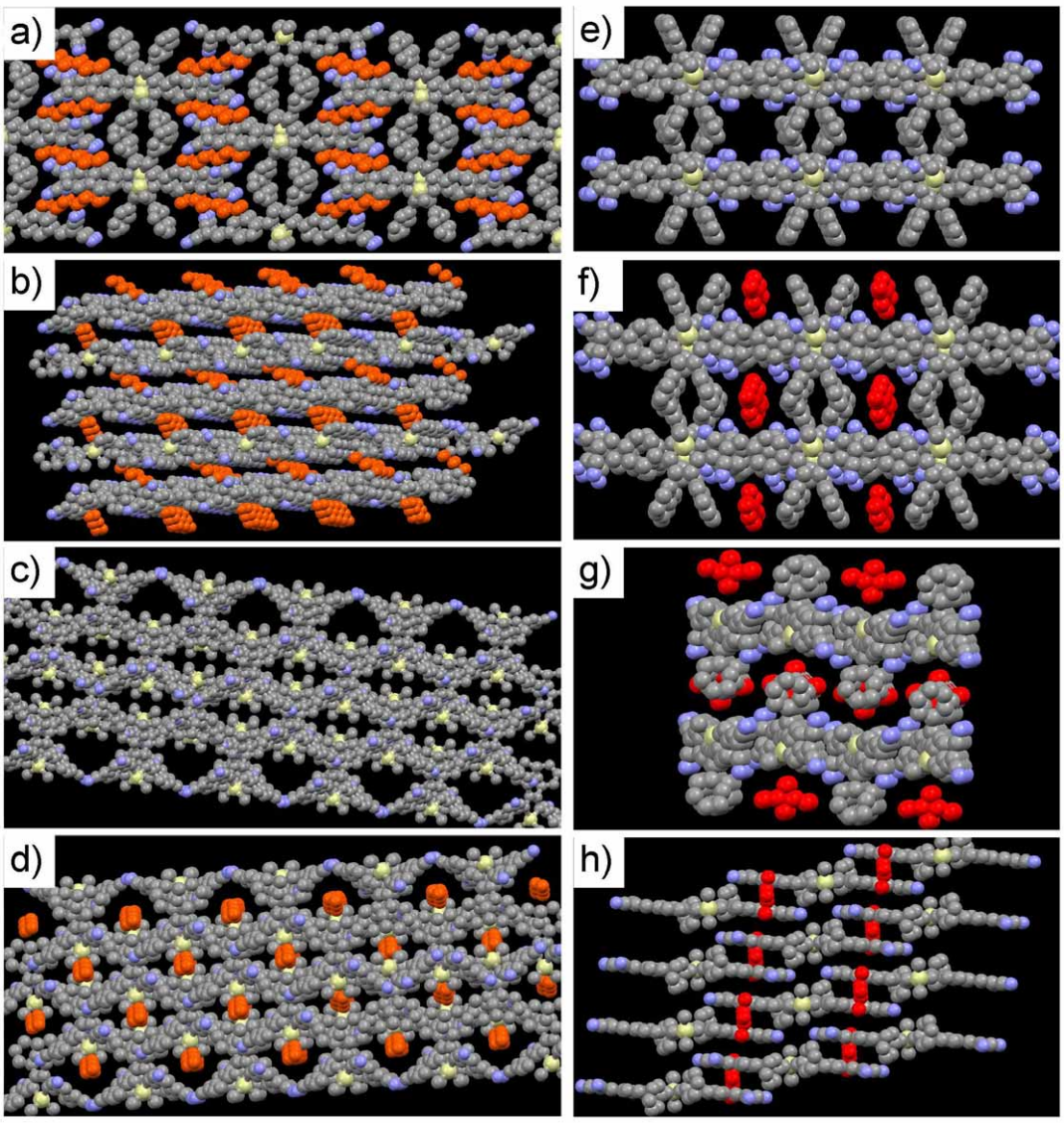

Fig. S8 Structures of crystal O and R. Panels a), b), c), and d) show the packing mood of molecule **8** and hexane in crystal O. a) a perspective view in the direction of *c* axis. b) A perspective view of the lattice to display the two groups of hexane molecules in a herringbone-like arrangement tilted to *a* axis. c) and d) are perspective views of crystal O excluding and including guest hexane molecules from an azimuth angle of –45° to *a* axis. Panels e), f), g), and h) show the packing mood of molecule **8** and acetone in crystal R. e) and f) are perspective views of crystal R excluding and including guest acetone molecules from an azimuth angle of *c* axis. (g) A perspective view of crystal R containing acetone molecules along axis *a*, and (h) is perspective view of crystal R including acetone molecules along axis *b*. The crystal structures are displayed in space-filling presentation. Hydrogen atoms were omitted in all of the graphs. For the host frameworks, C, N, and Si atoms are shown in grey, light purple and light yellow, respectively. For guest molecules, the skeletons of hexane and acetone molecules are shown in orange and red, respectively.

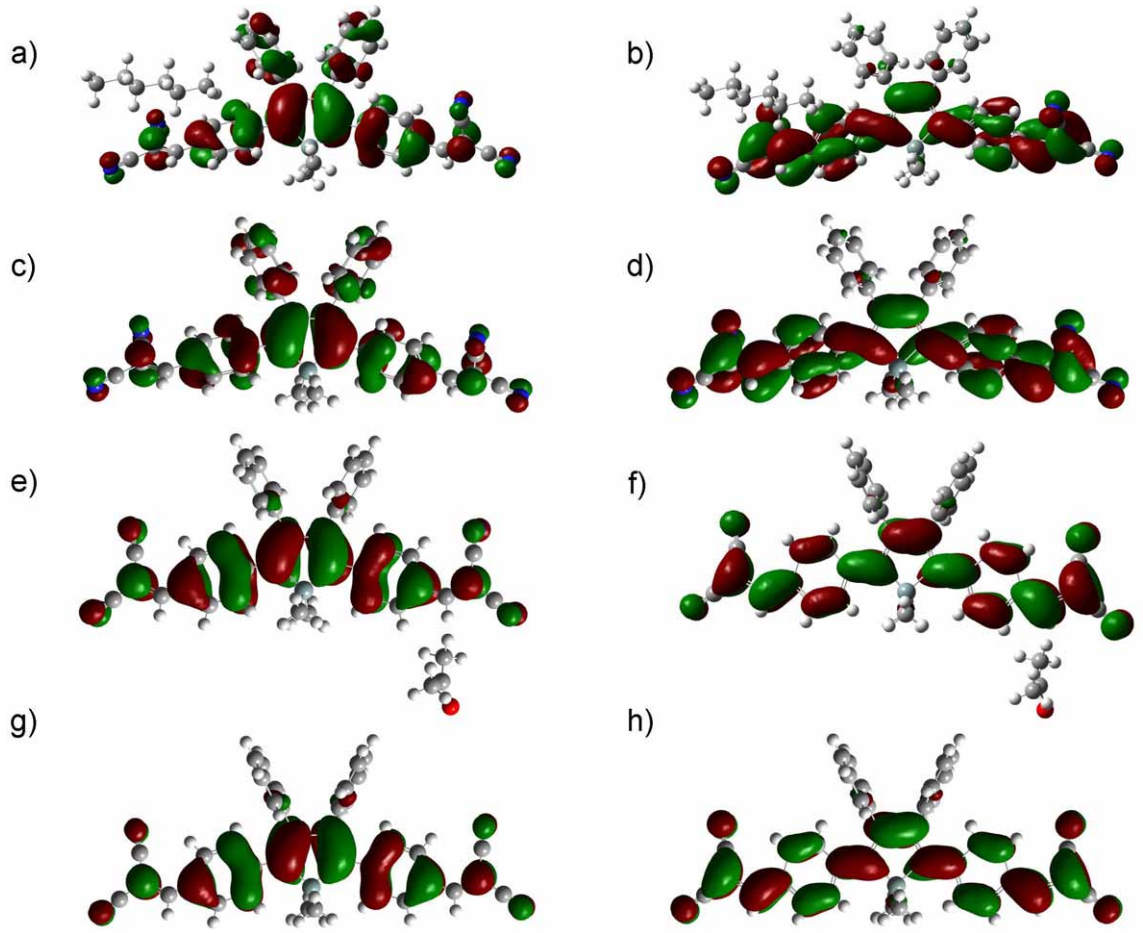

Fig. S9 Representative frontier orbitals of molecule **8** in crystal O and R.[S1] a) and b) display the LUMO and HOMO orbitals for molecule **8** in crystal O including hexane molecule; while c) and d) for those excluding hexane molecule. e) and f) display the LUMO and HOMO orbitals for molecule **8** in crystal R including acetone molecule; while g) and h) for those excluding acetone. The orbital configurations indicate that the guest molecules have no electronic interactions with the host molecule **8**.

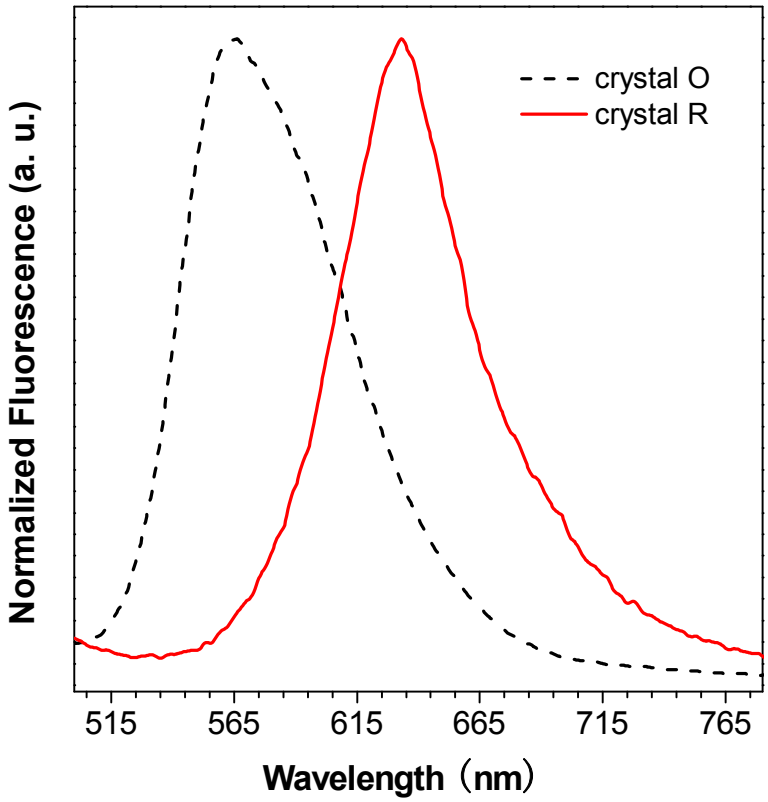

Fig. S10 Fluorescence spectra of molecule **8** in crystal O and R (λ_{ex} = 429 nm).

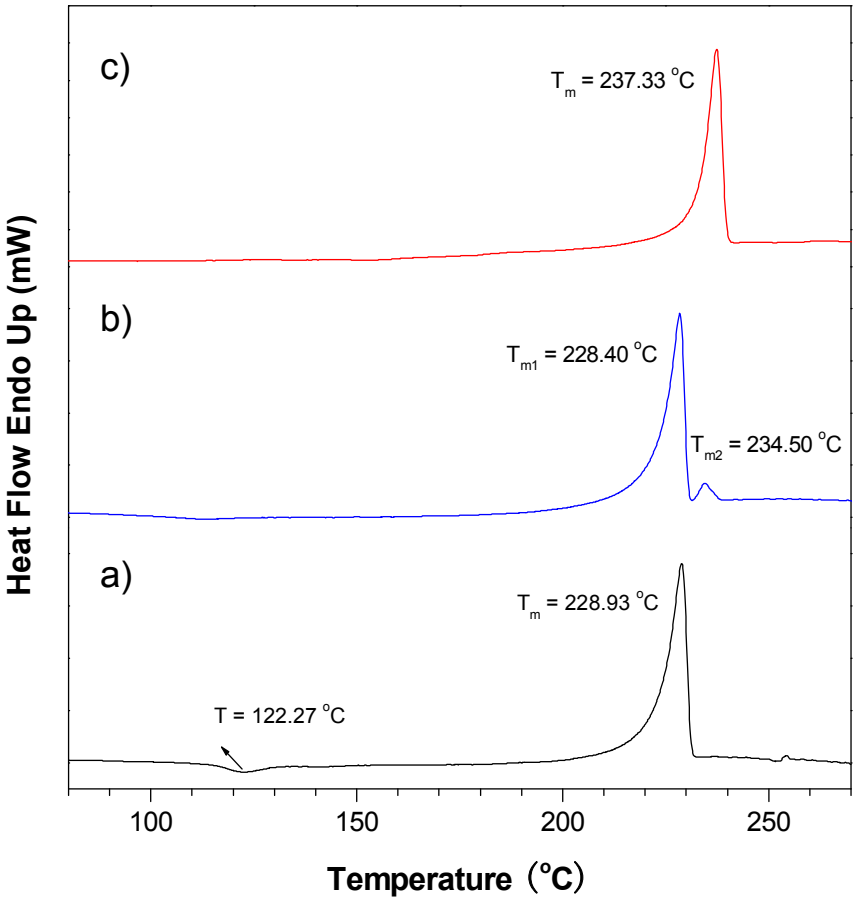

Fig. S11 DSC curves of different solids of molecule **8** (scanning rate: 10 K/min, atmosphere: N_2), (a) O-form (before grinding), (b) R-form (after grinding) and (c) YO-form (after heating).

Table S1. Crystal Data and Structure Refinement for Crystal O and R.

	O	**R**
Empirical formula	C_{44} H_{40} N_4 Si	C_{41} H_{32} N_4 O Si
Formula weight	652.89	624.80
Temperature	133(2) K	173(2) K
Wavelength	1.54178 Å	1.54178 Å
Crystal system	Monoclinic	Monoclinic
Space group	C2/c	P2/c
Unit cell dimensions	a=30.7917(4) Å α= 90° b=10.2374(1) Å β=90.4810(10)° c=11.7082(2) Å γ= 90°	a=13.268(3) Å α= 90° b=10.287(2) Å β=113.39(3)° c=13.771(4) Å γ= 90°
Volume	3690.61(9) $Å^3$	1725.2(7) $Å^3$
Z	4	2
Density (calculated)	1.175 Mg/m^3	1.203 Mg/m^3
Absorption coefficient	0.828 mm^{-1}	0.889 mm^{-1}
F(000)	1384	656
Crystal size	0.38 x 0.25 x 0.10 mm^3	0.35 x 0.28 x 0.05 mm^3
Theta range for data collection	2.87 to 67.49°.	10.08 to 67.50°.
Index ranges	-22<=h<=36,-10<=k<=12, -13<=l<=10	-12<=h<=15,-12<=k<=12, -16<=l<=12
Reflections collected	6043	5512
Independent reflections	3269 [R(int) = 0.0139]	3033 [R(int) = 0.0507]
Completeness to theta=66.50°	98.4 %	97.3 %
Absorption correction	Semi-empirical from equivalents	Semi-empirical from equivalents
Max. and min. transmission	1.00 and 0.81	1.00 and 0.90
Refinement method	Full-matrix least-squares on F2	Full-matrix least-squares on F2
Data / restraints / parameters	3269 / 0 / 224	3033 / 3 / 208
Goodness-of-fit on F2	1.036	1.003
Final R indices [I>2sigma(I)]	R1 = 0.0366, wR2 = 0.1015	R1 = 0.0562, wR2 = 0.1091
R indices (all data)	R1 = 0.0396, wR2 = 0.1043	R1 = 0.0950, wR2 = 0.1175
Largest diff. peak and hole	0.371 and –0.194 $e.Å^{-3}$	0.472 and –0.439 $e.Å^{-3}$

References

(S1) also see reference 14 in the main text of the manuscript.

Gaussian 09 (Revision A.02), M. J. Frisch, G. W. Trucks, H. B. Schlegel, G. E. Scuseria, M. A. Robb, J. R. Cheeseman, G. Scalmani, V. Barone, B. Mennucci, G. A. Petersson, H. Nakatsuji, M. Caricato, X. Li, H. P. Hratchian, A. F. Izmaylov, J. Bloino, G. Zheng, J. L. Sonnenberg, M. Hada, M. Ehara, K. Toyota, R. Fukuda, J. Hasegawa, M. Ishida, T. Nakajima, Y. Honda, O. Kitao, H. Nakai, T. Vreven, J. A. Montgomery, J. E. Peralta, Jr., F. Ogliaro, M. Bearpark, J. J. Heyd, E. Brothers, K. N. Kudin, V. N. Staroverov, R. Kobayashi, J. Normand, K. Raghavachari, A. Rendell, J. C. Burant, S. S. Iyengar, J. Tomasi, M. Cossi, N. Rega, J. M. Millam, M. Klene, J. E. Knox, J. B. Cross, V. Bakken, C. Adamo, J. Jaramillo, R. Gomperts, R. E. Stratmann, O. Yazyev, A. J. Austin, R. Cammi, C. Pomelli, J. W. Ochterski, R. L. Martin, K. Morokuma, V. G. Zakrzewski, G. A. Voth, P. Salvador, J. J. Dannenberg, S. Dapprich, A. D. Daniels, O. Farkas, J. B. Foresman, J. V. Ortiz, J. Cioslowski and D. J. Fox, Gaussian, Inc., Wallingford CT, 2009.